JOURNAL OF OPTOELECTRONICS AND ADVANCED MATERIALS Vol. 8, No. 2, April 2006, p. 455 - 460

Section 1. Perovskites

Investigation of chemical and grain boundary effects in highly ordered Sr_2FeMoO_6: XPS and Mössbauer studies

M. RAEKERS[a,*], K. KUEPPER[a,d], H. HESSE[a], I. BALASZ[b], I. G. DEAC[b], S. CONSTANTINESCU[c], E. BURZO[b], M. VALEANU[c], M. NEUMANN[a]
[a]*Dept. of Physics, University of Osnabrück, D-49069 Osnabrück, Germany*
[b]*Faculty of Physics, Babes-Bolyai University, 3400, Cluj-Napoca, Romania*
[c]*National Institute of Materials Physics, P.O. Box MG-07, Bucharest, Romania*
[d]*Institut für Ionenstrahlphysik und Materialforschung, Forschungszentrum Rossendorf, 01314 Dresden, Germany*

We have studied the oxidation states of Fe and Mo and the presence of grain boundaries in the magneto resistive (MR) compounds Sr_2FeMoO_6 by means of x-ray photoelectron spectroscopy (XPS), Mössbauer spectroscopy and electrical resistivity measurements. XPS of the Mo 3*d* and Fe 3*s* core levels is indicating a mixed valence state involving around 30% Fe^{3+}- Mo^{5+} and 70% Fe^{2+}- Mo^{6+} states. Mössbauer studies confirm the presence of a valence fluctuation state and an essential amount of grain boundaries in the present Sr_2FeMoO_6 crystals. Resistivities and magnetoresistance studies evidenced strong grain boundary effects.

(Received January 18, 2006; accepted March 23, 2006)

Keywords: Sr_2FeMoO_6, Double perovskite, Magnetoresistance, X-ray photoelectron spectroscopy, Mössbauer spectroscopy, Electrical resistivity

1. Introduction

Since the discovery of large magnetoresistance (MR) in Sr_2FeMoO_6, double perovskites have attracted much attention [1]. More strictly speaking, Sr_2FeMoO_6 is a tunnelling magneto resistance compound, with conductivity driven by the tunnelling of the charge carriers across insulating barriers [2,3]. The high Curie temperature, T_c = 420 K, and an essential MR present also at room temperature make this material to be an interesting candidate for possible applications, e. g. as magnetic switch or in the growing field of spintronics. However, the development of a thorough understanding of these fascinating magnetic and electronic transport properties of Sr_2FeMoO_6 is complicated due to different reasons. For instance the valence states of Fe and Mo have been studied by different experimental and theoretical approaches, leading to quite different results. A number of works conclude that a Fe^{3+}-Mo^{5+} configuration is present in Sr_2FeMoO_6 [4-6]. However, other investigations also suggested a Fe^{2+}-Mo^{6+} configuration or mixed Fe and Mo valence states [7-10]. The technique of core level x-ray photoelectron spectroscopy can be used to investigate the chemical properties of the compound in question. This method is element specific and sensitive to the valence state of the different constituents of the material (chemical shift). Furthermore one gets valuable information about hybridisation effects, here in particular about charge transfer between iron and the oxygen ligands.

Another interesting question is whether there exists a kind of electron hopping or valence fluctuation between the Fe and Mo sites, or if the ions have a fixed charge. Such a valence fluctuation state has been observed before, for instance in Fe_3O_4 or $BaSmFe_2O_{5+u}$ [11]. Linden et al. also found indications for valence fluctuations in Sr_2FeMoO_6 [7]. Besides the properties of the Fe and Mo ions the properties of Sr_2FeMoO_6 are strongly influenced by structural properties such as so called antisite defects. This means Mo ions are randomly replaced by Fe ions and vice versa. Based on the false-site imperfection model, the saturation magnetisation of Sr_2FeMoO_6 is decreasing with an increasing amount of anti site defects [12].

Another interesting effect that may occur in transition metal oxides is the formation of anti phase boundaries or grain boundaries. It is much more difficult to investigate grain boundaries than antisite defects. The latter ones can be easily analysed by x-ray diffraction (XRD), whereas grain boundaries are very difficult to detect or even invisible for XRD. However, recently such grain boundaries in Sr_2FeMoO_6 have been investigated by means of Mössbauer spectroscopy and resistivity measurements [13,14]. Also grain boundaries are suspected to play an essential role for the magneto resistance in Sr_2FeMoO_6 by building up insulating barriers, which are, at least to large extent, responsible for the tunnelling magneto resistance. The investigation of the hyperfine interactions between the nucleus with its surrounding environment by means of Mössbauer spectroscopy is suitable to investigate the effects mentioned above.

In order to understand the intricate interplay between the Fe and Mo ions, antisite defects and grain boundaries in Sr_2FeMoO_6 we present a study of the chemical (valence states, charge transfer) and grain boundary effects in a

highly ordered Sr_2FeMoO_6 crystals by means of the complementary techniques x-ray photoelectron and ^{57}Fe Mössbauer spectroscopy. In addition, magnetoresistivity studies were also performed.

2. Experimental details

Polycrystalline samples of Sr_2FeMoO_6 were produced by standard solid state reaction. The samples were prepared from $SrCO_3$,Fe_2O_3 and MoO_3 by milling, pressing and two subsequent heating cycles in air. Afterwards sample 3.1 was heated at 1300 ^oC under argon flow with 1.7 % hydrogen, whereas in case of sample 3.3 the hydrogen content was only 0.8 %.. X-ray diffraction (XRD) was used to check the structural quality and it was found that the sample 3.1 has only a very low antisite defect (AS) concentration of ≅3%. A total magnetic moment of 3.5 μ_B/f.u. was determined by magnetic measurements. The sample 3.3 having ≅ 5 % antisites was also studied. The saturation moment was 3.3 μ_B/f.u.. Some information of the structural, electronic and magnetic properties were reported elsewhere [10,15]. The XPS measurements were performed with a PHI 5600ci multi-technique spectrometer with monochromatic Al K_α radiation, giving an overall resolution of about 0.4 eV. The spectrometer was calibrated using an Au foil as a reference sample (the binding energy of the Au $f_{7/2}$ core level is 84.0 eV). To get a surface free of contaminations, the sample was fractured in situ. The ^{57}Fe Mössbauer spectra were recorded at 77 K and room temperature. A ^{57}Co:Rh source was used for the measurements. The conventional four probe method was used for resistivity measurements in temperature range 4 K ≤ T ≤ 300 K. The magnetoresistance was measured in field up to μ_0H = 7 T.

3. Results and discussion

One can probe the valence state of iron in transition metal compounds by studying the Fe 3s x-ray photoelectron spectra for sample 3.1 (Fig. 1, bottom panel). Applying a phenomenological model [16], the spectral splitting of the 3s core-level x-ray photoemission spectra in transition metals and their compounds originates from the exchange coupling between the 3s hole and the 3d electrons, and is modified by configuration interaction. The magnitude of the splitting is related to (2S + 1), where S is the local spin of the 3d electrons in the ground state. FeO ($3d^6$ configuration) shows an exchange splitting of around 5.4 eV whereas the 3s splitting in Fe_2O_3 ($3d^5$ configuration) is 6.4 eV. The XPS Fe 3s spectrum of the double perovskite shows a splitting of around 5.7 eV. Assuming a linear relationship between exchange splitting and ratio of valence state, this leads to the conclusion that around 30% of the Fe ions are in the +3 valence state. Additionally, a satellite at higher binding energies which we assign to charge transfer excitations is visible. Compared to the spectra of FeO and Fe_2O_3 we find an intermediate amount of charge transfer excitations in Sr_2FeMoO_6.

The Mo 3d XPS spectrum (Fig. 1a) comprises two rather broad peaks located at around 232 eV and 235 eV on a binding energy scale. In order to separate the obviously overlapping Mo^{5+} and Mo^{6+} states one can de-convolute the spectrum with help of Doniach-Sunjic functions [19]. The features which can be associated with Mo^{5+} contributions (dashed lines) show a rather pronounced tail (asymmetry) to higher binding energies (~ 25%). The analysis of the peak areas after background subtraction reveals 29% Mo^{5+} and 71% Mo^{6+} contributions to the Mo 3d spectrum, in very good concurrence with the result for the iron. The two rather small fitted peaks located at around 229.6 eV and 233 eV are likely due to surface defect states because firstly, the Fe 3s spectrum also shows a weak shoulder on the low binding energy side, and secondly, similar effects of surface defects on XPS spectra have been investigated in other studies of transition metal compounds, such as TiO [20] or WoO_3 [21].

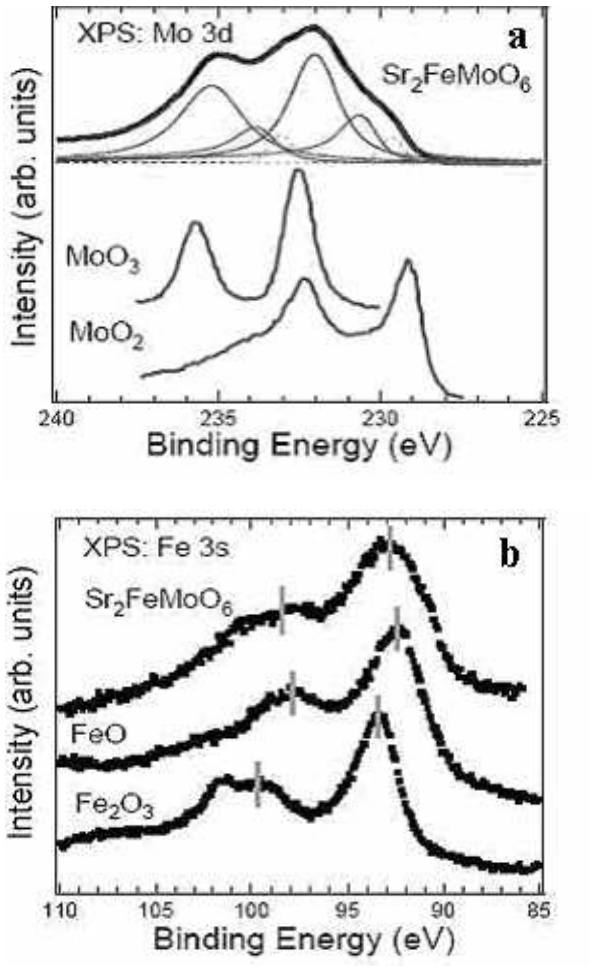

Fig. 1. XPS core level spectra of Mo 3d (a) and Fe 3s (b) of Sr_2FeMoO_6 (sample 3.1) compared with the spectra of some benchmark compounds, the Fe 3s spectrum of FeO has been taken from Prince et al. [17], the Mo 3d spectra of MoO_2 and MoO_3 have been adapted from Colton et al. [18].

Since the photoelectron emission event is very fast and occurs at the femtosecond scale it is not possible to extract the information if the ions have a fixed charge or a valence fluctuation state is present. In case of valence fluctuation the electron hopping occurs at a timescale of nanoseconds, and the fast photoelectron emission process is like a very short "snapshot". On the other side the Mössbauer event takes place at a timescale of ~10^{-7} seconds and is essentially slower than a possible electron hopping process. If the Fe ions would have a fixed charge, a Mössbauer spectrum would comprise two distinct features representing the Fe^{2+} and the Fe^{3+} ions, whereas a valence fluctuation state would lead to one component in the Mössbauer spectrum which is due to the average valence state of the iron.

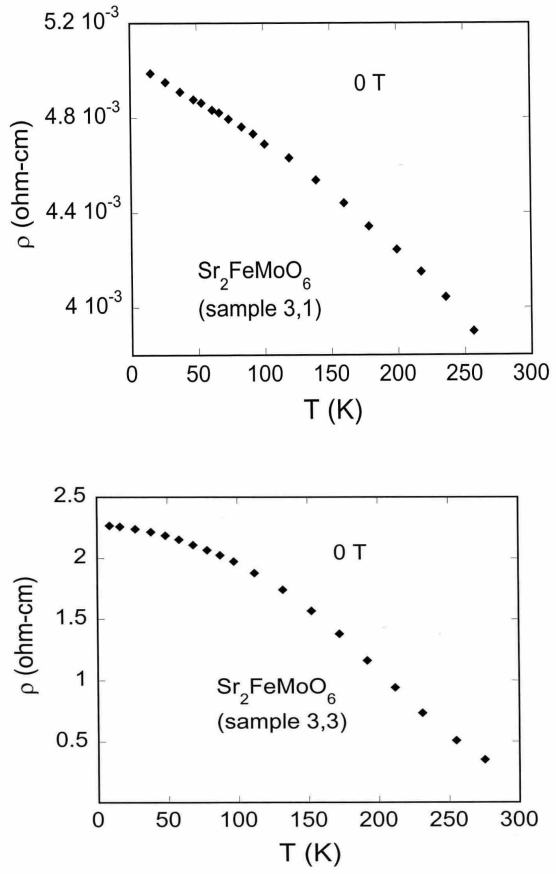

Fig. 2. Temperature dependences of the resistivities in field H = 0.

The temperature dependences of the electrical resistivities for samples 3.1 and 3.3, in zero external field, are plotted in Fig. 2. The residual resistivity of the sample 3.3 is higher by more than three order of magnitude than of the sample 3.1. The resistivities decrease when increasing temperature. Negative magnetoresistances (MR) are evidenced in both samples. At 9 K, the MR values for sample 3.1 change by 14 % in field of 1 T and 30 % at 7 T. The field dependences of resistivity are smaller in case of sample 3.3, being 9 % in field of 1 T and 20 % in external field of 7 T. At 250 K, the magnetoresistances are nearly the same as at 9 K for sample 3.1 but for sample 3.3 is below 1 % - Fig. 3. This behaviour may be correlated with recent results [22] where the antisite defects versus grain boundary competition in tunnelling magnetoresistance of Sr_2FeMoO_6 was discussed. Analysing comparatively the resistivities of samples 3.1 and 3.3, we conclude that the differences in resistivities of the above samples may be connected only with grain boundary properties. The tunnelling magnetoresistance response is deteriorated when the grain boundary insulating barriers are present. Although, in our case, the antisite proportions are rather close for the both samples, as above mentioned, there are high changes in resistivities. Generally, it is expected that in more disordered sample there is a reduced electron spin polarization at the Fermi level which influence the resistivities. But this cannot be considered to be responsible for a more than three order of magnitude difference between the resistivities of the above samples. We assume that the tunnelling magnetoresistance of sample 3.3 is masked by the grain boundary barriers.

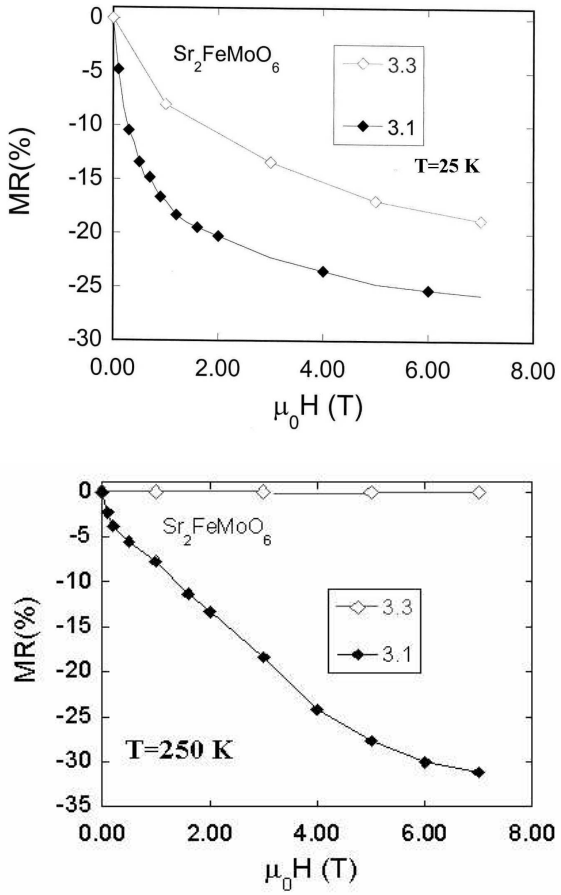

Fig. 3. Field dependences of the magnetoresistivities at 25 K and 250 K.

The samples 3.1 and 3.3 were analysed by Mössbauer spectroscopy. The ^{57}Fe Mössbauer spectra at 77K are plotted in Fig. 4. The spectrum of sample 3.1 was

decomposed in four sextets - Fig. 4a. The hyperfine parameters are close to those determined by Linden et al [13], although the area ratios are different – Table 1. According to previous data [7,13,23], the component M1 with an internal field of 46 T was attributed to iron residing in mixed valence state Fe^{2+}/Fe^{3+} at right sites. Component AS with an internal field more than ≅ 50T is assigned to Fe^{3+} ions located in antisites. The sextet M2 with an internal field of ≅ 48T arises from iron ions adjacent to AS iron. These ions are considered to be in mixed valence state. The component APB having low internal field may be attributed to trivalent iron in antiphase domain boundary (APB) The antisite (AS) content is 5.8 % and the iron adjacent to antisite (M2 component) is 18.8 %. We note that the antisite content agree rather well with the value determined by XRD. The area ratios between M2 and AS components, both in the present study and that of Linden et al [13] is ≅ 3. It seems to be a constant number, in the mean, for the ratio between the number of iron adjacent atoms to an antisite and antisite content. The component having the smaller hyperfine (APB) has an area A = 3.9 %, much smaller than 21 % reported previously [13].

The ^{57}Fe Mössbauer spectrum of sample 3.3 was analysed, considering in the central region of the spectrum, the presence of two quadrupole doublets (Fig. 4b) or one sextet with small hyperfine field (Fig. 4c). The parameters of both fits are listed in Table 1. In the first case we have two sextes with nearly the same isomer shifts and quadrupole splittings, but with little different ^{57}Fe hyperfine fields (46.8 and 48.5 T). The sextet with B_{hf}=46.8 T was attributed to iron in M1 sites. It seems unrealistic to attribute the sextet with hyperfine field of 48.5 T only to M2 type sites since the number of ions around AS positions is too high. Probably that this sextet include also the contributions of a fraction of iron situated in M1 sites Since of complexity of spectrum it seems to be an unrealistic decomposition for this subspectrum. This fact can take into account the higher area rations of M2/AS than 3.0 evidenced already. The fraction of iron located in antisite is 3.30 %, in good agreement with that determined by XRD refinement. Two quadrupole doublets evidenced in the central part (A ≅ 6.8 %) can originate from superparamagnetic particles having blocking temperature smaller than 80 K and situated at the grain boundaries.

In another type of analysis, the hyperfine parameters follow a trends close to that reported for sample 3.1. The sextet with ^{57}Fe hyperfine field of 59.5 T was attributed to iron located in antisites. This internal field is higher than the value determined in sample 3.1 but also characterizes the hyperfine field of Fe^{3+} ions. The area ratio is 6.2 % little higher than 5 % determined by XRD analysis. The Mössbauer spectrum of Sr_2FeMoO_6, at 4.2 K, was analysed already by considering four doublets having hyperfine ≅48.2 T (61%); 50 T (≅13%); 52.5 T (15%) and 55.4 T (11%) [24]. The first three components were attributed to iron having a configuration $3d^{5+\delta}$ with decreasing δ values as the B_{hf} values increase and the component with 55.4 T was attributed to Fe^{3+} ions. We note that in FeF_3 a value of B_{hf}=62.3 T was determined. The fraction of iron located in APB is 6.5% close to 6.8 % evidenced in first type of analysis but nearly two time higher than determined in sample 3.1. The M1 component was analysed considering two contributions (M1' and M1") with different hyperfine fields 46.9 and 50.7 T, respectively. The origin of M1' sextet is not clear. Probably in some regions of samples there is no random distribution of iron in the two valence states. As a result a fluctuating valence more close to Fe^{3+} iron configuration may be present.

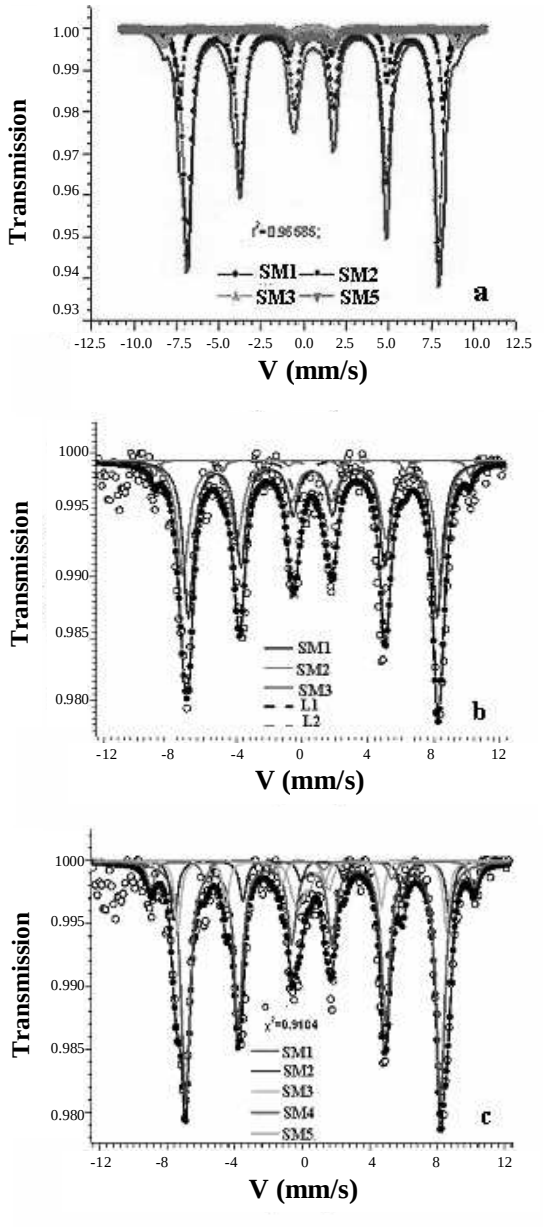

Fig. 4. Mössbauer spectrum of Sr_2FeMoO_6 recorded at 77K: (a) sample 3.1; (b,c) sample 3.3 The spectrum in (b) has been de-convoluted into three sextets, and two doublets. The spectrum in (c) has been de-convoluted into five sextets. The hyperfine components are summed up in Table 1.

Table 1. Hyperfine parameters obtained from the fits of the ^{57}Fe Mössbauer spectra.

Sample	Lattice	δ_{Rh} (mm/s)	$eQV_{ZZ}/8$ (mm/s)	Θ^o	Γ (mm/s)	B (T)	A (%)
(sample 3.1)	M1	0.573	-0.049	133.5	0.55	45.8	71.52
χ^2=0.97	M2	0.440	-0.200	58.6	0.42	48.3	18.78
	AS	0.439	-0.025	130.6	0.61	54.0	5.82
	SM5 (APB)	0.522	0.085	113.5	0.42	8.4	3.88
(sample 3.3)	SM1 (M1)	0.64	≅0.000	125	0.37	46.8	48.79
χ^2=0.87	SM2 (M2+M1)	0.57	0.004	119	0.43	48.5	41.11
	SM3 (AS)	0.65	0.020	120	0.25	59.4	3.30
	L1 (APB)	-0.33	-	-	0.41	-	3.69
	L2 (APB)	1.42	-	-	0.48	-	3.11
(sample 3.3)	SM1 (M1')	0.60	0.640	126	0.32	46.9	62.47
χ^2=0.91	SM2 (M1")	0.88	-0.278	148	0.24	50.7	12.26
	SM3 (M2)	0.33	-0.415	69	0.21	49.4	12.58
	SM4 (AS)	0.19	0.698	137	0.27	59.5	6.19
	SM5 (APB)	0.30	0.298	149	0.27	5.7	6.50

The present data for sample 3.3 may be interpreted considering a strong grain surface oxidation at the grain boundaries. The content of APB is higher than in sample 3.1 in agreement with the resistivity studies. This fact may be correlated with sample preparation. Probably that the low hydrogen content in the argon flow leads to a stronger oxidation of grain boundaries than for sample 3.1. It is not excluded to be present also a charge ordering as suggested by the presence of M1' and M1" sextets for iron located in normal positions.

4. Conclusions

In summary, we have investigated highly ordered Sr_2FeMoO_6 samples by core level XPS and Mössbauer spectroscopy. By comparing the Fe 3s and Mo 3d XPS spectra with spectra of reference compounds we can conclude mixed iron and molybdenum valence states involving around 30% Fe^{3+}- Mo^{5+} and 70% Fe^{2+}- Mo^{6+} states. The analysis of the Fe 3s spectrum reveals that charge transfer between the Fe 3d states and the O 2p ligands plays a role, and de-convoluting the Mo 3d spectrum reveals metallic character of the Mo^{5+} ions. Furthermore, the ^{57}Fe Mössbauer spectra indicate the presence of valence fluctuations, an electron jumps from a Fe^{2+} ion to a Mo^{6+} ion leading to a Fe^{3+}-Mo^{5+} configuration, and vice versa. Analysing the hyperfine field parameters of the Mössbauer data supports the results obtained by XPS, the iron in the bulk is more divalent than trivalent. The grain boundary play an important role in determining the resistivity and magnetoresistivities of Sr_2FeMoO_6. The tunnelling magnetoresistance may be masked by the grain boundary barriers as in sample (3.3) where the grain boundary content is rather high. For samples having high resistivities no magnetoresitive effect was observed close to room temperature. The atomic resolution TEM measurements [24], showed in Sr_2FeMoO_6, the presence of domain with modulated crystal structure inside the regions of the ideal double perovskite. These regions with cation disorder form insulating domains in the half-metallic matrix of the ordered double perovskite. These insulating regions can also contribute to changes in resistivities of the samples (3.3) as suggested by Mössbauer effect data where M1' and M1" components were shown.

Acknowledgements

Financial support by the PhD program of Lower Saxony, Germany, and by the Graduate College 695 of Deutsche Forschungsgemeinschaft and Federal State of Lower Saxony, Germany, is gratefully acknowledged. Financial support in framework of CERES Programe C-361 is gratefully acknowledged in performing XRD, resistivities and Mössbauer effect studies.

References

[1] K. L. Kobayashi, T. Kimura, H. Sawada, K. Terakura, Y. Tokura, Nature **395**, 677 (1998).
[2] T. Saitoh, N. Nakatake, A. Kakizaki, H. Nakajima, O. Moritomo, Sh Xu, Y. Moritomo, N. Hamada, Y. Aiura, Phys. Rev. B **66**, 035112 (2002).
[3] A. Deb, N. Hiraoka, M. Ituo, Y. Sakurai, A. Koizumi, Y. Tomioka, Y. Tokura, Phys. Rev. B **70**, 104411 (2004).
[4] T. Nakawaga, J. Phys. Soc. Jpn. **24**, 806 (1968).
[5] D. D. Sarma, P. Mahadevan, T. Saha-Dasgupta, S. Ray, A Kumar, Phys. Rev. Lett. **85**, 2549 (2000).
[6] S. Ray, A. Kumar, D. D. Sarma, R. Cimino, S. Turchini, S. Zennaro, N. Zema, Phys. Rev. Lett. **87**, 097204 (2001).
[7] J. Linden, T. Yamamoto, M. Karppinen, H. Yamauchi, T. Pietari, Appl. Phys. Lett. **76**, 2925 (2000).
[8] A. P. Douvalis, M. Venkatesan, J. M. D. Coey, M. Grafoute, J. M. Greneche, R. Suryanarayanan, J. Phys: Condens.Matter **14**, 12611 (2002).
[9] M. Besse, V. Cros, A. Barthélémy, H. Jaffrès, J. Vogel, F. Petroff, A. Mirone, A. Tagliaferri, P. Bencok, P. Decorse, P. Berthet, Z. Szotek, W. M. Temmerman, S. S. Dhesi, N. B. Brookes, A. Rogalev, A. Fert, Europhys. Lett. **60**, 608 (2002).

[10] K. Kuepper, I. BalaszI, H. Hesse, A. Winiarski, K. C. Prince, M. Matteucci, D. Wett, R. Szargan, E. Burzo, M. Neumann, Phys. Status Solidi a **201** 3252 (2004).
[11] J. Lindén, P. Karen, A. Kjekshus, J. Miettinen, T. Pietari, M. Karppinen, Phys. Rev. B **60**, 15251 (1999).
[12] L. Balcells, J. Navarro, M. Bibes, A. Roig, B. Martinez, J. Fontcuberta, Appl. Phys. Lett. **78**, 781 (2000).
[13] J. Lindén, M. Karppinen, T. Shimada, Y. Yasukawa, H. Yamauchi, Phys. Rev. B **68**, 174415 (2003).
[14] D. Niebieskikwiat, F. Prado, A. Caneiro, R. D. Sánchez, Phys. Rev. **70**, 132412 (2004).
[15] K. Kuepper, M. Kadiroglu, A. V. Postnikov, K. C. Prince, M. Matteucci,V. R. Galakhov, H. Hesse, G. Borstel, M. Neumann, J. Phys.: Condens. Matter **17**, 4309 (2005).
[16] V. R. Galakhov, M. Demeter, S. Bartkowski, M. Neumann, N. A. Ovechkina, E. Z. Kurmaev, N. I. Lobachevskaya, Ya. M. Mukovskii, J. Mitchell, D. L. Ederer, Phys. Rev. B **65**, 113102 (2002).
[17] K. C. Prince, M. Matteucci, K. Kuepper, S. G. Chiuzbaian, S. Bartkowski, M. Neumann, Phys. Rev. B **71**, 085102 (2005).
[18] R. J. Colton, A. M. Guzman, J. W. Rabalais, J. Appl. Phys. **49**, 409 (1978).
[19] S. Doniach, M. Sunjic J. Phys. C: Solid State Phys. **3**, 285 (1970).
[20] S. Bartkowski, M. Neumann, E. Z. Kurmaev, V. V. Federenko, S. N. Shamin, V. M. Cherkashenko, S. N. Memnonov, A. Winiarski, D. C. Rubie, Phys. Rev. B **56**, 10656 (1997).
[21] C. Cantalini, L. Lozzi, A. Passacantando, S. Santucci, IEEE Sensors Journal **3,** 171 (2003).
[22] D. Niebieskikwait, F. Prado, A. Caneiro, R. D. Sanchez, Phys. Rev. B **70**, 132412 (2004).
[23] J. M. Greneche, M. Venkatesan, R. Suryanarayanan, J. M. D. Coey, Phys. Rev. B **63,** 174403 (2001).
[24] Z. Klencsár, Z. Németh, A. Vértes, I. Kotsis, M. Nagy, Á. Cziráki, C. Ulhaq-Bouillet, V. Pierron-Bohnes, K. Vad, S. Mészáros, J. Hakl, J. Magn. Magn. Mat **281**, 115 (2004).

*Corresponding author: michael.raekers@uos.de